AJNR

Susceptibility-Weighted Imaging of the Pediatric Brain after Repeat Doses of Gadolinium-Based Contrast Agent

K. Ozturk and D. Nascene

AJNR Am J Neuroradiol published online 22 April 2021
http://www.ajnr.org/content/early/2021/04/22/ajnr.A7143

Published April 22, 2021 as 10.3174/ajnr.A7143

Susceptibility-Weighted Imaging of the Pediatric Brain after Repeat Doses of Gadolinium-Based Contrast Agent

K. Ozturk and D. Nascene

ABSTRACT

BACKGROUND AND PURPOSE: Gadolinium complexes have paramagnetic properties; thus, we aimed to determine the susceptibility changes in the globus pallidus and dentate nucleus following administration of linear or macrocyclic gadolinium-based contrast agents in children.

MATERIALS AND METHODS: Thirty-three patients with linear gadolinium-based contrast agent gadopentetate dimeglumine administration, 33 age- and sex-matched patients with macrocyclic gadolinium-based contrast agent gadobutrol administration, and 33 age- and sex-matched control subjects without gadolinium exposure were enrolled in this retrospective study. The signal intensity on SWI and T1WI was determined in the dentate nucleus, middle cerebellar peduncle, globus pallidus, and pulvinar of the thalamus in an ROI-based analysis to calculate dentate nucleus–to–middle cerebellar peduncle and globus pallidus–to–thalamus ratios. A repeated measures ANOVA was performed to compare $SWI_{minimum}$, SWI_{mean}, and T1WI signal intensity ratios between gadolinium-based contrast agent groups and control subjects. Pearson correlation analysis was performed to determine any correlation between signal intensity ratios and variables.

RESULTS: Dentate nucleus–to–middle cerebellar peduncle and globus pallidus–to–thalamus ratios for both SWI_{mean} and $SWI_{minimum}$ were lower for the linear gadolinium-based contrast agent group compared with macrocyclic gadolinium-based contrast agent and control groups ($P < .05$). No significant difference of the SWI_{mean} and $SWI_{minimum}$ ratios were noted between the macrocyclic gadolinium-based contrast agent group and the control group ($P > .05$). Both dentate nucleus–to–middle cerebellar peduncle and globus pallidus–to–thalamus ratios on T1WI in the linear gadolinium-based contrast agent group were higher than in the control group and the macrocyclic gadolinium-based contrast agent group ($P < .05$). A negative correlation was identified between SWI_{mean} and $SWI_{minimum}$ ratios and the number of linear gadolinium-based contrast agent administrations (dentate nucleus–to–middle cerebellar peduncle ratio: SWI_{mean}, $r = -0.43$, $P = .005$; $SWI_{minimum}$, $r = -0.38$, $P = .011$; globus pallidus–to–thalamus ratio: SWI_{mean}, $r = -0.39$, $P = .009$; $SWI_{minimum}$, $r = -0.33$, $P = .017$).

CONCLUSIONS: SWI analysis of the pediatric brain demonstrated a statistically significant decrease in $SWI_{minimum}$ and SWI_{mean} values for the dentate nucleus and globus pallidus after administration of linear gadolinium-based contrast agents but not macrocyclic gadolinium-based contrast agents.

ABBREVIATIONS: DN = dentate nucleus; GBCA = gadolinium-based contrast agent; GP = globus pallidus; MCP = middle cerebellar peduncle; min = minimum; SI = signal intensity; Th = pulvinar of the thalamus

Gadolinium-based contrast agents (GBCAs) are essential components of clinical diagnosis and treatment decision-making for millions of patients worldwide.[1] Recent studies have shown gadolinium deposition in multiple organs,[2] including the brain, after repeat administration of GBCAs.[3] Intracranial gadolinium deposition in the brain has been associated with increased signal intensity (SI) on T1WI,[4] most notably in the globus pallidus (GP) and cerebellar dentate nucleus (DN).[5] Substantial evidence has been provided by histopathologic analysis indicating that the reported T1WI SI increase in the DN and GP corresponds to gadolinium deposition.[6]

SI changes in the brain parenchyma on unenhanced T1-weighted MR imaging have been identified in association with various histopathologic processes.[7] Particularly, hyperintensity within the DN on T1WI due to shortening of the T1 relaxation time is believed to occur secondary to several factors, including ferric iron accumulation, ferritin accumulation associated with lipid

Received August 6, 2020; accepted after revision December 17.

From the Department of Radiology, University of Minnesota, Minneapolis, Minnesota.

Please address correspondence to Kerem Ozturk, MD, Division of Neuroradiology, Department of Radiology, University of Minnesota, B-226 Mayo Memorial Building, MMC 292, 420 Delaware St SE, Minneapolis, MN 55455; e-mail: oztur027@umn.edu ; @keremozturk_rad

http://dx.doi.org/10.3174/ajnr.A7143

Table 1: Exclusion criteria

Exclusion Parameters	Control Group	Macrocyclic GBCA Group	Linear GBCA Group
Initially selected	57	64	61
Age younger than 2 years	3	5	6
Renal dysfunction	2	0	0
Hepatic dysfunction	3	2	2
Lesion in the cerebellum, midbrain, corpus striatum, or pulvinar of the thalamus	3	2	1
Missing documentation of the prior contrast agent	8	11	7
Missing or unsatisfactory T1WI	2	2	3
Missing or unsatisfactory SWI	3	4	3
Different sequences and parameters between comparison T1WIs	0	5	6
Final No. of groups	33	33	33

peroxidation, and the presence of paramagnetic free radicals as well as paramagnetic compounds like metal ions such as iron and manganese.[8,9] Any of these histopathologic mechanisms could play a role in the T1WI SI observed in the DN and GP of patients with gadolinium retention. Recently, numerous studies have focused on the association between increased SI on unenhanced T1WI and exposure to intravenously administered GBCAs.[10]

SWI is a high-resolution 3D gradient-echo sequence that incorporates phase and magnitude data to identify variations in magnetic susceptibility between adjacent tissues with a sensitivity greater than conventional gradient-echo sequences.[11] Its higher sensitivity in the detection of paramagnetic and diamagnetic compounds such as iron particles, blood-breakdown products, and calcifications provides clinically relevant information in the assessment of various conditions, including neurodegeneration, cerebral neoplasm, vascular malformation, and intracranial hemorrhage.[12] Because gadolinium has a paramagnetic effect, SWI can be used for noninvasive visualization of gadolinium retention within the DN and GP that may not be apparent by T1WI.[13]

In this study, we hypothesized that sequential use of GBCAs would increase the magnetic susceptibility within the DN and GP as seen on SWI. Thus, we analyzed the susceptibility values in the DN and GP of children who had consecutive applications of the linear GBCA gadopentetate dimeglumine or the macrocyclic GBCA gadobutrol compared with control subjects who had no history of GBCA administration.

MATERIALS AND METHODS

All procedures were performed in accordance with the ethical standards of the institutional research committee and with the 2013 revised Helsinki declaration and its later amendments or comparable ethical standards. This study was approved by the local institutional review board and the requirement to obtain informed consent was waived.

Patients

This was a retrospective single-center study of children and adolescents (age at final contrast-enhanced MR imaging examination younger than 18 years) who underwent brain MR imaging with administration of the macrocyclic GBCA gadobutrol or the linear GBCA gadopentetate dimeglumine between 2010 and 2020. Before January 1, 2014, a linear GBCA, gadopentetate dimeglumine (Magnevist; Bayer HealthCare Pharmaceuticals), was used at our institution for nearly all brain MR imaging examinations. Since January 1, 2014, our institution changed to the macrocyclic GBCA gadobutrol (Gadavist; Bayer Schering Pharma). This allowed us to have a population of children who had acquired only the macrocyclic GBCA gadobutrol to compare with a similar earlier population who had received only the linear GBCA gadopentetate dimeglumine. We retrospectively screened our database to identify children who met the following inclusion criteria: 1) the patients' ages ranged from 2 to 18 years, 2) MR imaging follow-up was performed exclusively in our department, and 3) contrast-enhanced MR imaging with the exclusive use of the macrocyclic GBCA gadobutrol or the linear GBCA gadopentetate dimeglumine was followed by another 3T MR imaging including unenhanced T1WI and SWI. The lower limit of 2 years of age was selected to exclude younger children with possible incomplete myelination.[13] Exclusion criteria were the following: 1) renal insufficiency; 2) liver dysfunction; 3) missing data or unsatisfactory image quality of unenhanced T1WI and/or SWI; 4) structural brain abnormality in the cerebellum, midbrain, corpus striatum, or pulvinar of the thalamus (Th), determined by the study investigators at the time of retrospective image review; and 5) broadly varying MR imaging parameters among the MR imaging scans (>5% for TR or >10% for TE). The exclusion criteria of the study design are shown in Table 1. In total, 33 patients with exclusive use of linear GBCAs and 33 age- and sex-matched patients receiving macrocyclic GBCAs were finally enrolled in this study.

A total of 33 control subjects matched for age and sex were selected for each case patient and consisted of pediatric patients who underwent nonenhanced brain MR imaging between 2010 and 2020 without any record of GBCA administration.

Clinical Data

Data on demographics were acquired from a standardized review of the health records of all children through a radiology search. For all included patients, age, sex, intrinsic disease, and number and type of GBCA administrations, along with the accumulated GBCA dose and history of chemotherapy or radiation therapy, were assessed by chart review (Table 2).

The number of macrocyclic GBCA and linear GBCA administrations was abstracted from the medical charts. The macrocyclic GBCA gadobutrol and the linear GBCA gadopentetate dimeglumine were dosed at 0.1 mmol per kilogram of the patient's body weight.

Table 2: Clinical and radiologic characteristics of the study population[a]

Characteristic	Linear GBCA–Exposed Children	Macrocyclic GBCA–Exposed Children	GBCA-Naive Control Subjects
Age (yr)			
Mean (SD)	8.2 (SD, 5.4)	8.2 (SD, 5.1)	8.2 (SD, 3.6)
Range	2–18	2–18	2–18
Sex			
Male	23	23	23
Female	10	10	10
Mean (SD) No. of contrast-enhanced MR imaging	2.4 (SD, 2.4)	4.03 (SD, 2.9)	0
Mean (SD) time interval between MR imaging (mo)	7.16 (SD, 7.5)	7.4 (SD, 7.3)	0
Mean (SD) accumulated gadolinium dose (mmol)	17.5 (SD, 24.1)	13.3 (SD, 11.9)	0
Diagnosis			
Intracranial neoplasm	7	7	10
Extracranial neoplasm	2	0	1
Pituitary abnormality	3	6	2
Orbit/optic nerve pathology	6	7	2
Adrenoleukodystrophy	5	5	10
Benign conditions	10	8	8
History of radiation treatment	3	2	3
History of chemotherapy	6	5	4
History of neurosurgery	2	2	3

[a] Data are number of patients unless indicated otherwise and mean (SD).

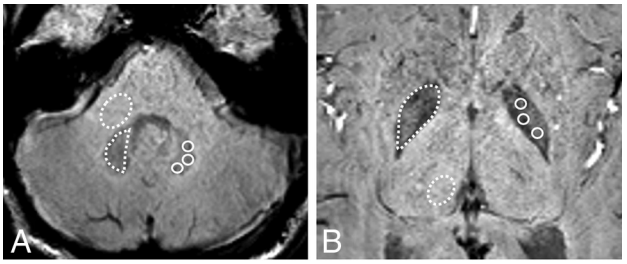

FIG 1. SWI at the level of the DN (*A*) and GP (*B*) used for drawing the ROIs in the DN and GP with the corresponding MCP and Th for normalization, respectively. *Dotted lines* illustrate the freehand ROI used to obtain SWI_{mean} from the DN, GP, MCP, and Th; *solid lines* illustrate the circular ROIs used to obtain SWI_{min} from the DN and GP.

Image Acquisition

All examinations were performed on 3T MR imaging scanners (Tim Trio and Magnetom Skyra; Siemens) with 16- or 20-channel head coils. The scanning sequences included the conventional MR images and SWI. The parameters for conventional MR images were as follows: FLASH T1WI before and after GBCA injection (TR, 250 ms; TE, 2.48 ms; section thickness, 2.0 mm; FOV, 250 mm), fast spin-echo T2WI (TR, 6000 ms; TE, 99 ms; section thickness, 2.0 mm; section interval, 1.0 mm; FOV, 250 mm), FLAIR T2WI (TR, 9000 ms; TE, 81 ms; TI, 2400 ms; section thickness, 2.0 mm; section interval, 1.0 mm; FOV, 250 mm).

All patients underwent precontrast SWI scanning (TR, 27 ms; TE, 20 ms; flip angle, 15; bandwidth, 250 kHz; matrix size, 256 × 134; parallel factor, 2; FOV, 250 mm; and acquisition time, approximately 2 minutes and 30 seconds). Presaturation slabs were used to saturate air-containing structures such as the petrous pyramids and paranasal sinuses. SWI was performed as a 1-mm isotropic 3D acquisition with minimum intensity projections of the SWI, and images were reconstructed on an axial plane with a 2-mm section thickness.

ROI Analysis

Image analysis of unenhanced T1WI was performed as described in detail previously by Kanda et al[14] and replicated in other reports on studies of brain gadolinium deposition. Placement of ROIs was performed by a neuroradiology fellow (K.O.), who was blinded to the clinical data. The images were also reviewed independently by a second radiologist (D.N.) with 10 years of experience in neuroradiology for the correct placement of the ROIs into the DN, middle cerebellar peduncle (MCP), GP, and Th. The DN and GP were selected because they are commonly analyzed regions of T1WI SI hyperintensity in the brain after GBCA administration.[14-16] Also, McDonald et al[17] reported that the DN contains the highest concentration of gadolinium deposition in the brain tissue of deceased patients.

ROI placement and subsequent image-based analysis was performed using a dedicated software, Vitrea (Vital Images). Freehand ROIs were drawn within both the DN and GP; then, an elliptic ROI was placed in MCP and Th, respectively, on SWI to determine SWI_{mean} SI ratios with an average of 3 measurements. $SWI_{minimum\ (min)}$ was extracted from the manual placement of at least 5 circular ROIs into the DN and GP that encompassed 5 voxels (approximately 5 mm^2), and the lowest value was determined (Fig 1). Compatible with the previous study,[18] SI ratios were calculated as follows: T1WI ratio = (T1WI SI of DN)/(T1WI SI of MCP) or (T1WI SI of GP) / (T1WI SI of Th); SWI_{mean} ratio = (SWI_{mean} of DN) / (SWI_{mean} of MCP) or (SWI_{mean} of GP) / (SWI_{mean} of Th); and SWI_{min} ratio = (SWI_{min} of DN) / (SWI_{mean} of MCP) or (SWI_{min} of GP) / (SWI_{mean} of Th). Eventually, all ROIs were visually inspected for correctness to modify possible structural displacement from baseline due to suboptimal coregistration.

Statistics

Data were tested for normality using the Shapiro-Wilk test, and the choice of parametric-versus-nonparametric tests was made on the basis of the outcome of this test. We conducted a repeated measures ANOVA with post hoc Bonferroni tests for pair-wise multiple comparisons for the DN-to-MCP and GP-to-Th ratios on unenhanced T1WI and SWI among the following: 1) only macrocyclic GBCA administration in the GBCA group versus the non-GBCA group; 2) only linear GBCA administration in the GBCA group versus the non-GBCA group; and 3) only macrocyclic GBCA administration in the GBCA group versus only linear GBCA administrations in the GBCA group. Pearson correlation

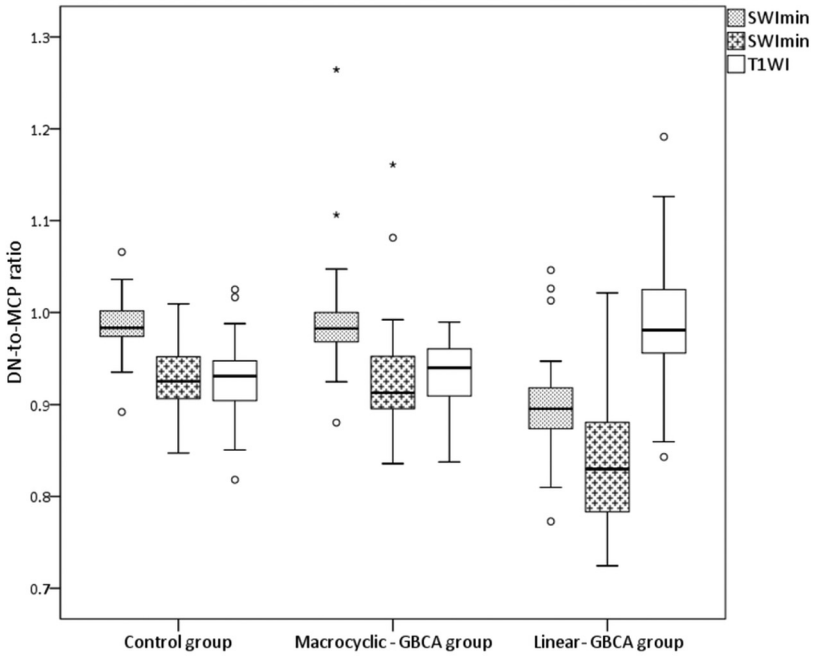

FIG 2. Boxplots of the mean DN-to-MCP ratios on SWI and T1WI among the linear GBCA, macrocyclic GBCA, and control groups. The *error bars* for boxplots represent the minimum and maximum data points within each group, and the *Middle box* represents the 25th, 50th, and 75th percentiles of the data within each group.

analyses were performed to evaluate associations between DN-to-MCP and GP-to-Th ratios from the most recent brain MR imaging examinations in patients exposed to GBCA and confounding parameters, including the number of MR images, total cumulative linear or macrocyclic GBCA dose, the mean duration between MR imaging, and age. The independent samples *t* test or 1-way ANOVA was used to assess the DN-to-MCP and GP-to-Th ratio difference in the GBCA-exposed groups according to sex, intrinsic disease, history of brain radiation therapy, and chemotherapy. Consequently, the variables that were found to be statistically different on univariate analyses were further subjected to multivariate linear regression analysis. Intraobserver agreement of reader 1 (K.O.) for the quantitative measurements of the SI ratio was determined with Lin concordance correlation coefficients. The a priori significance level was set to .05, and all reported *P* values are 2-tailed. A Bonferroni correction with an adjusted *P* value $< .05$ was considered statistically significant for 3-subgroup comparison. Analyses were performed using SPSS 23 for Windows (IBM).

RESULTS

Patient Characteristics

Our cohort included 33 children who had only the linear GBCA gadopentetate dimeglumine (mean age, 8.2 [SD, 5.4] years; range, 2–18 years), 33 sex- and age-matched children who had only the macrocyclic GBCA gadobutrol (mean age, 8.2 [SD, 5.1] years; range, 2–18 years), and 33 sex- and age-matched controls (mean age, 8.2 [SD, 3.6] years; range, 2–18 years). Patient characteristics and radiologic data are presented in Table 2. The mean number of doses of linear GBCA gadopentetate dimeglumine and macrocyclic GBCA gadobutrol were 2.4 (SD, 2.4) and 4.03 (SD, 2.9), respectively.

Intraobserver Agreement

The intraobserver agreement was substantial for T1WI values for both the DN-to-MCP ratio (Concordance correlation coefficient = 0.96; 95% CI, 0.92–0.98; $P < .001$) and the GP-to-Th ratio (Concordance correlation coefficient = 0.95; 95% CI, 0.91–0.98; $P < .001$); it was less concordant for SWI_{mean} and SWI_{min} for both the DN-to-MCP ratio (SWI_{mean}, Concordance correlation coefficient = 0.85; 95% CI, 0.79–0.90; $P = .003$; SWI_{min}, Concordance correlation coefficient = 0.83; 95% CI, 0.77–0.88; $P = .005$) and the GP-to-Th ratio (SWI_{mean}, Concordance correlation coefficient = 0.83; 95% CI, 0.78–0.89; $P = .004$; SWI_{min}, Concordance correlation coefficient = 0.82; 95% CI, 0.76–0.87; $P = .007$).

DN-to-MCP Ratio on SWI and T1WI

The DN-to-MCP ratios for SWI_{mean} and SWI_{min} were lower in those with only linear GBCA administration (SWI_{mean}, 0.898 [SD, 0.056]; SWI_{min}, 0.835 [SD, 0.073]) than in both the macrocyclic GBCA group (SWI_{mean}, 0.992 [SD, 0.061]; SWI_{min}, 0.928 [SD, 0.064]) and the control group (SWI_{mean}, 0.985 [SD, 0.032]; SWI_{min}, 0.925 [SD, 0.037]) (adjusted *P* value $< .001$). No significant differences in the DN-to-MCP ratio for SWI_{mean} and SWI_{min} were noted between the macrocyclic GBCA group and the control group ($P = .595$ and .829, respectively). The mean DN-to-MCP ratios on T1WI in the linear GBCA group (0.986 [SD, 0.073]) were also higher than those in the non-GBCA group (0.926 [SD, 0.042]) and the macrocyclic GBCA group (0.930 [SD, 0.043]) (adjusted *P* value $< .001$) (Fig 2). A moderate negative correlation was identified between the DN-to-MCP ratio for SWI_{mean} and SWI_{min} and the number of linear GBCA administrations (SWI_{mean}, $r = -0.43$ and $P = .005$; SWI_{min}, $r = -0.38$ and $P = .011$) (Fig 3).

The Pearson correlation coefficient revealed no significant correlation between SWI/T1WI–derived values and the mean time interval among MR imaging scans, total GBCA dose, and age (all $P > .05$). There was no significant difference in the SWI/T1WI–derived SI ratios regarding sex, intrinsic disease, and history of radiation or chemotherapy (all $P > .05$). Multivariate linear regression analyses derived from univariate analysis demonstrated that SWI_{mean} and SWI_{min} ratios were associated with the number of linear GBCA administrations (adjusted R^2 for the model = 0.227) (SWI_{mean}: regression coefficient $\beta = -0.026$, $P = .012$; SWI_{min}: $\beta = -0.03$, $P = .02$). Additionally, no significant correlation was noted between SWI-derived values and age in the control groups (SWI_{mean}: $r = -0.11$ and $P = .13$; SWI_{min}: $r = -0.15$ and $P = .20$).

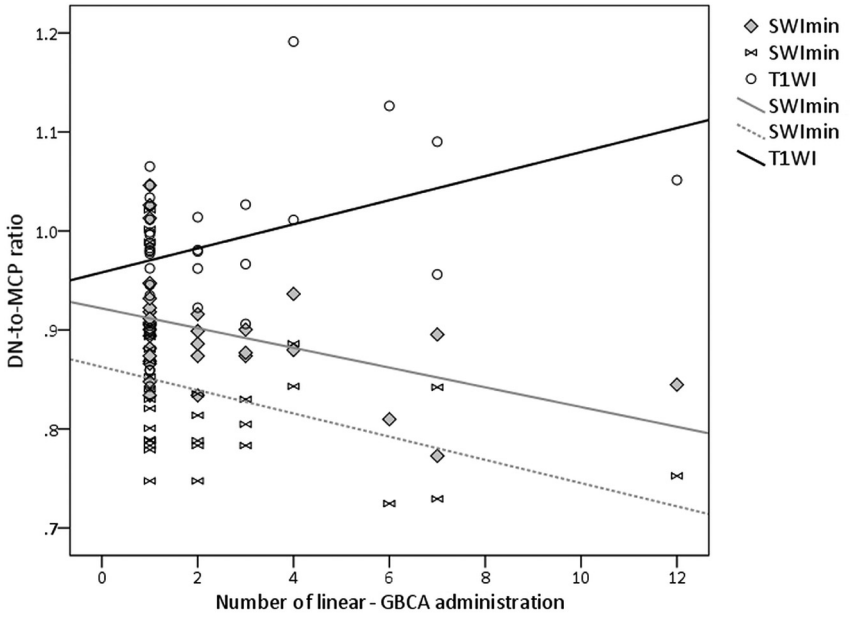

FIG 3. Scatterplot of the DN-to-MCP ratios for SWI_{mean}, SWI_{min}, and T1WI versus the number of intravenous linear GBCA administrations, with *linear regression lines* for each group.

Figure 4 demonstrates representative MR images. Figures 5 and 6 reveal scatterplots of the correlation between the DN-to-MCP ratios on unenhanced T1WI and SWI.

GP-to-Th Ratio on SWI and T1WI

The GP-to-Th ratios for SWI_{mean} and SWI_{min} were lower in those with only linear GBCA administration (SWI_{mean}, 0.765 [SD, 0.041]; SWI_{min}, 0.751 [SD, 0.038]) than in both the macrocyclic GBCA group (SWI_{mean}, 0.804 [SD, 0.047]; SWI_{min}, 0.793 [SD, 0.045]) and the control group (SWI_{mean}, 0.857 [SD, 0.052]; SWI_{min}, 0.841 [SD, 0.048]) (adjusted P value $<$ .001). No significant differences of the GP-to-Th ratio for SWI_{mean} and SWI_{min} were noted between the macrocyclic GBCA group and the control group ($P = .503$ and 0.778, respectively). Mean GP-to-Th ratios on T1WI in the linear GBCA group (1.001 [SD, 0.072]) were also higher than in the non-GBCA group (0.953 [SD, 0.047]) and the macrocyclic GBCA group (0.958 [SD, 0.049]) (adjusted P value $<$ .001). A moderate negative correlation was identified between the GP-to-Th ratio for SWI_{mean} and SWI_{min} and the number of linear GBCA administrations (SWI_{mean}, $r = -0.39$, $P = .009$; SWI_{min}, $r = -0.33$, $P = .017$).The Pearson correlation coefficient revealed no significant correlation between SWI/T1WI–derived values and the mean time interval among MR imaging, total GBCA dose, and age (all $P > .05$). There was no significant difference in the SWI/T1WI–derived SI ratios regarding sex, intrinsic disease, and a history of radiation or chemotherapy (all $P > .05$). Multivariate linear regression analyses derived from univariate analysis demonstrated that SWI_{mean} and SWI_{min} ratios were associated with the number of linear GBCA administrations (adjusted R^2 for the model = 0.185) (SWI_{mean}; $\beta = -0.022$, $P = .015$; SWI_{min}; $\beta = -0.026$, $P = .028$). Additionally, no significant correlation was noted between SWI-derived values and age in the control groups (SWI_{mean}: $r = -0.14$, $P = .15$; SWI_{min}: $r = -0.11$, $P = .24$).

DISCUSSION

In this study, we aimed to determine whether administration of the macrocyclic GBCA gadobutrol or the linear GBCA gadopentetate dimeglumine in children is correlated with the development of a susceptibility signal within the DN or GP as an imaging surrogate for gadolinium deposition. The DN-to-MCP and GP-to-Th ratios for SWI_{mean} and SWI_{min} in children who received only linear GBCAs were lower than those in the non-GBCA group (control group) and macrocyclic GBCA group. On T1WI, previous reports have shown a strong relationship between the hyperintensity in the DN/GP and linear GBCA administration;[16] our results also reinforce the previous results.

The clinical relevance of intracranial gadolinium retention, if any, remains unknown. Nevertheless, the pediatric brain may be more prone to the deleterious effects of gadolinium deposition because the pediatric brain is typically more susceptible to a number of toxins.[19,20] Additionally, the cumulative dose and duration of exposure to GBCAs may be greater in children than in adults.[20] Thus, it is essential to determine the safest GBCAs for the pediatric population.[21] Recent studies investigating pediatric intracranial gadolinium deposition have concentrated on the linear GBCA gadopentetate dimeglumine,[22] though a few studies in the pediatric population have analyzed the effect of repeat administration of macrocyclic GBCAs.[23] Radbruch et al[24] and Ryu et al[15] examined the sequential administration of the macrocyclic GBCA gadoterate meglumine in pediatric patients and found that this agent was not correlated with T1WI hyperintensity in the DN. In addition, Tibussek et al[23] analyzed a group of pediatric patients receiving repeat administration of the macrocyclic GBCAs gadoteridol and gadoterate meglumine and did not observe any T1WI hyperintensity within the DN.

The DN and GP are known to have a rich iron content, and a high susceptibility signal within DN and GP has been reported previously due to its paramagnetic potency.[25] The magnitude SI on SWI depends on T2*, geometry, orientation to the B_0, and differences in magnetic susceptibility, as well as serving as a function of T1.[11] If additional gadolinium is deposited in the DN, SI values on SWI should theoretically decrease after serial GBCA administration because gadolinium is a strong paramagnetic substance with a molar susceptibility of 325 ppm L/mol.[26] In this study, the susceptibility values in the DN and GP were better correlated with the number of linear GBCA administrations than T1WI SI ratios were. One explanation for a stronger association between susceptibility values and the number of linear GBCA administrations is that the endogenous substances cause susceptibility changes in the DN and GP but induce less T1 shortening.[7] This explanation conflicts with the results of Hinoda et al,[26] which demonstrated that the susceptibility values on quantitative susceptibility mapping in the DN correlated

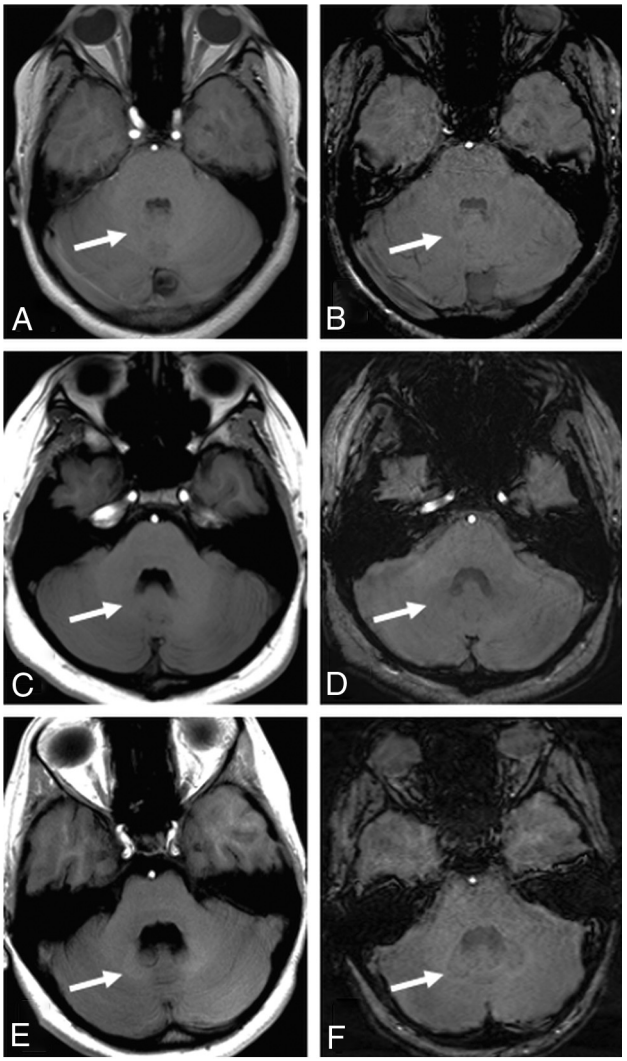

FIG 4. A 13-year-old male patient without gadolinium exposure (*A* and *B*), an age- and sex-matched patient after 5 doses of macrocyclic GBCA (*C* and *D*), and another 13-year-old adolescent boy after 7 doses of linear GBCA administration (*E* and *F*). Note the brighter signal in the DN on T1WI (*E*) and lower signal in the DN on SWI (*F*), which is not present in the other 2 children. (*White arrows* represent DN)

worse with the number of linear GBCA administrations than T1 ratios did. The reason for the difference in results between the study by Hinoda et al[26] and our present study could be partially explained by the potential washout effect or precipitation of gadolinium[27] after consecutive administration of linear and macrocyclic GBCAs because the GBCA group in their study had both linear and macrocyclic GBCA administration. Additionally, we used a matched case-control design in a pediatric population, given that age-dependent maturational effects in different areas of the developing brain may cause SI changes on SWI with time. A better correlation of the number of linear GBCA administrations and susceptibility values in the DN and GP than T1WI SI ratios supports the initial hypothesis that SWI could be a biomarker of gadolinium retention in vivo and could better depict gadolinium deposition compared with T1WI.

SWI is an imaging approach that maximizes sensitivity to susceptibility effects by integrating a long-TE, fully flow-compensated, 3D gradient-echo series with filtered phase data in each voxel to improve the contrast in magnitude images. This limitation is being addressed with the recent development of quantitative susceptibility mapping.[28] While SWI generates contrast on the basis of phase images, quantitative susceptibility mapping further computes the underlying susceptibility of each voxel as a scalar quantity and may be better for evaluating subtle susceptibility signal changes related to the possible gadolinium deposition in the brain parenchyma.[29]

The SI changes on SWI occur from both T2 and susceptibility signal variations among tissues and are very sensitive to the in vivo detection of iron deposition.[30] In a previous postmortem study,[31] the DN demonstrated varying signal intensity on SWI; in particular, the susceptibility values of the DN significantly changed due to iron deposition with aging.[32] In this study, the result of the Pearson correlation coefficient between the susceptibility values in DN or GP and subject age revealed no significant correlation in this pediatric population. Furthermore, no significant correlation was noted between SWI-derived values and age in the control groups, which might need a larger patient cohort and larger age range with possible involvement of the adult population. However, in a time (eg, 2–3 years) in which age-related changes are minimal, SWI appears to provide a means to monitor gadolinium deposition in the DN due to its quantitative nature and high gadolinium sensitivity.

There were some limitations to this retrospective study investigating the relationship between SWI and gadolinium deposition in the DN and GP. First, the number of GBCA administrations has been obtained from medical charts at a single institution, and some patients with long-term follow-up in the GBCA group might have had additional GBCA exposure at outside facilities of which we were not aware in this analysis. Second, a larger number of control subjects could have been included to minimize the error in the control data; however, in this regard, an increased number of control subjects would technically decrease the variance between the patients receiving GBCA and the control subjects, which could potentially disclose other significant variations between the 2 groups. Third, a possible limitation in all DN SI-change studies is the choice of the proper comparator. We considered the DN-to-MCP ratio because it has been used in other studies and the anatomic position of the DN is closer to the MCP compared with the pons, allowing collection of all ROIs on the same section, which might be beneficial in case of regional variances in the images. We conducted a case-control design because as fiber maturation and associated SWI/T1WI signal changes develop in a nonlinear way and demonstrate considerable variability, modeling of these effects would be very complicated. Also, histologic analyses of brain tissue samples are likely even more sensitive for detecting lower-level gadolinium deposition that may not be detectable on SWI.[33]

CONCLUSIONS

This study demonstrated a statistically significant decrease in SWI_{min} and SWI_{mean} values for the DN and GP after consecutive administrations of linear GBCA but not macrocyclic GBCA in pediatric patients.

Disclosures: David Nascene—*UNRELATED*: *Consultancy*: WorldCare Clinical; *Payment for Lectures Including Service on Speakers Bureaus*: Biogen; *Royalties*: Springer. *Money paid to individual author.

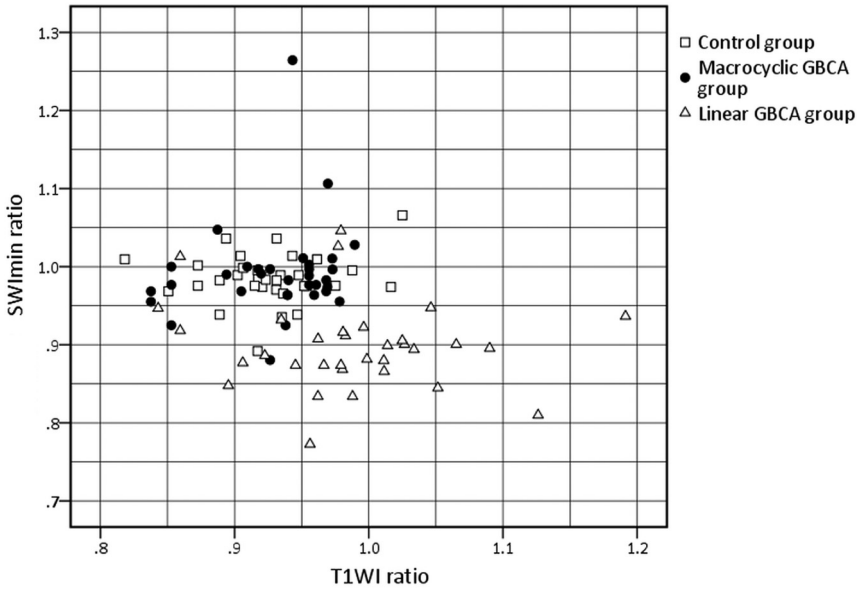

FIG 5. Scatterplot of the DN-to-MCP ratios on unenhanced T1WI and SWI. Increased T1WI and decreased SWI_{mean} ratios in the linear GBCA group compared with macrocyclic GBCA and control groups are seen.

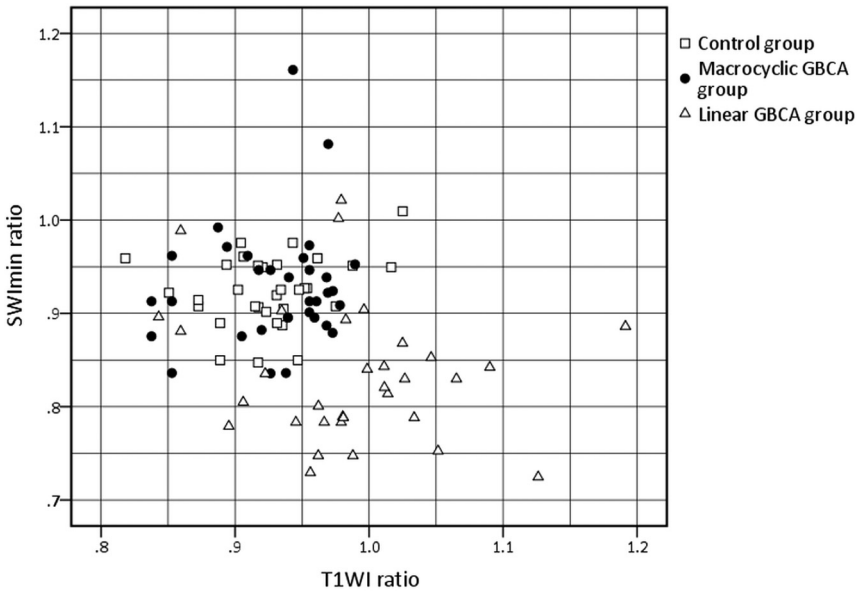

FIG 6. Scatterplot of the DN-to-MCP ratios on unenhanced T1WI and SWI. Note increased T1WI and decreased SWI_{min} ratios in the linear GBCA group compared with macrocyclic GBCA and control groups.

REFERENCES

1. Boehm I, Hungerbuhler M, Heverhagen JT. **Insight into the dynamic of gadolinium based contrast agent (GBCA) hypersensitivity: acquisition, persistence and disappearance.** *Magn Reson Imaging* 2018;49:1–3 CrossRef Medline
2. Khawaja AZ, Cassidy DB, Al Shakarchi J, et al. **Revisiting the risks of MRI with gadolinium-based contrast agents: review of literature and guidelines.** *Insights Imaging* 2015;6:553–58 CrossRef Medline
3. Choi JW, Moon WJ. **Gadolinium deposition in the brain: current updates.** *Korean J Radiol* 2019;20:134–47 CrossRef Medline
4. Rossi Espagnet MC, Bernardi B, Pasquini L, et al. **Signal intensity at unenhanced T1-weighted magnetic resonance in the globus pallidus and dentate nucleus after serial administrations of a macrocyclic gadolinium-based contrast agent in children.** *Pediatr Radiol* 2017;47:1345–52 CrossRef Medline
5. Tedeschi E, Palma G, Canna A, et al. **In vivo dentate nucleus MRI relaxometry correlates with previous administration of gadolinium-based contrast agents.** *Eur Radiol* 2016;26:4577–84 CrossRef Medline
6. McDonald RJ, McDonald JS, Kallmes DF, et al. **Intracranial gadolinium deposition after contrast-enhanced MR imaging.** *Radiology* 2015;275:772–82 CrossRef Medline
7. Tamrazi B, Nguyen B, Liu CJ, et al. **Changes in signal intensity of the dentate nucleus and globus pallidus in pediatric patients: impact of brain irradiation and presence of primary brain tumors independent of linear gadolinium-based contrast agent administration.** *Radiology* 2018;287:452–60 CrossRef Medline
8. Valdés Hernández M, Maconick LC, Tan EMJ, et al. **Identification of mineral deposits in the brain on radiological images: a systematic review.** *Eur Radiol* 2012;22:2371–81 CrossRef Medline
9. Ginat DT, Meyers SP. **Intracranial lesions with high signal intensity on T1-weighted MR images: differential diagnosis.** *Radiographics* 2012;32:499–516 CrossRef Medline
10. Young JR, Orosz I, Franke MA, et al. **Gadolinium deposition in the paediatric brain: T1-weighted hyperintensity within the dentate nucleus following repeated gadolinium-based contrast agent administration.** *Clin Radiol* 2018;73:290–95 CrossRef Medline
11. Haacke EM, Mittal S, Wu Z, et al. **Susceptibility-weighted imaging: technical aspects and clinical applications, Part 1.** *AJNR Am J Neuroradiol* 2009;30:19–30 CrossRef Medline
12. Nandigam RN, Viswanathan A, Delgado P, et al. **MR imaging detection of cerebral microbleeds: effect of susceptibility-weighted imaging, section thickness, and field strength.** *AJNR Am J Neuroradiol* 2009;30:338–43 CrossRef Medline
13. El-Koussy M, Schenk P, Kiefer C, et al. **Susceptibility-weighted imaging of the brain: does gadolinium administration matter?** *Eur J Radiol* 2012;81:272–27 CrossRef Medline
14. Kanda T, Ishii K, Kawaguchi H, et al. **High signal intensity in the dentate nucleus and globus pallidus on unenhanced T1-weighted MR images: relationship with increasing cumulative dose of a gadolinium-based contrast material.** *Radiology* 2014;270:834–41 CrossRef Medline
15. Ryu YJ, Choi YH, Cheon JE, et al. **Pediatric brain: gadolinium deposition in dentate nucleus and globus pallidus on unenhanced T1-**

weighted images is dependent on the type of contrast agent. *Invest Radiol* 2018;53:246–55 CrossRef Medline
16. Moser FG, Watterson CT, Weiss S, et al. **High signal intensity in the dentate nucleus and globus pallidus on unenhanced T1-weighted MR images: comparison between gadobutrol and linear gadolinium-based contrast agents.** *AJNR Am J Neuroradiol* 2018;39:421–26 CrossRef Medline
17. McDonald RJ, McDonald JS, Kallmes DF, et al. **Gadolinium deposition in human brain tissues after contrast-enhanced MR imaging in adult patients without intracranial abnormalities.** *Radiology* 2017;285:546–54 CrossRef Medline
18. Ozturk K, Nas OF, Soylu E, et al. **Signal changes in the dentate nucleus and globus pallidus on unenhanced T1-weighted magnetic resonance images after intrathecal administration of macrocyclic gadolinium contrast agent.** *Invest Radiol* 2018;53:535– 40 CrossRef Medline
19. Lanphear BP. **The impact of toxins on the developing brain.** *Annu Rev Public Health* 2015;36:211–30 CrossRef Medline
20. Roberts DR, Chatterjee AR. **The critical need for pediatric and juvenile animal research addressing gadolinium retention in the developing body.** *Invest Radiol* 2019;54:72–75 CrossRef Medline
21. Runge VM. **Dechelation (transmetalation): consequences and safety concerns with the linear gadolinium-based contrast agents, in view of recent health care rulings by the EMA (Europe), FDA (United States), and PMDA (Japan).** *Invest Radiol* 2018;53:571–78 CrossRef Medline
22. Ichikawa S, Omiya Y, Onishi H, et al. **Linear gadolinium-based contrast agent (gadodiamide and gadopentetate dimeglumine)-induced high signal intensity on unenhanced T1-weighted images in pediatric patients.** *J Magn Reson Imaging* 2019;49:1046–49 CrossRef Medline
23. Tibussek D, Rademacher C, Caspers J, et al. **Gadolinium brain deposition after macrocyclic gadolinium administration: a pediatric case-control study.** *Radiology* 2017;285:223–30 CrossRef Medline
24. Radbruch A, Haase R, Kickingereder P, et al. **Pediatric brain: no increased signal intensity in the dentate nucleus on unenhanced T1-weighted MR images after consecutive exposure to a macrocyclic gadolinium-based contrast agent.** *Radiology* 2017;283:828–36 CrossRef Medline
25. Chai C, Yan S, Chu Z, et al. **Quantitative measurement of brain iron deposition in patients with haemodialysis using susceptibility mapping.** *Metab Brain Dis* 2015;30:563–71 CrossRef Medline
26. Hinoda T, Fushimi Y, Okada T, et al. **Quantitative assessment of gadolinium deposition in dentate nucleus using quantitative susceptibility mapping.** *J Magn Reson Imaging* 2017;45:1352–58 CrossRef Medline
27. Radbruch A, Weberling LD, Kieslich PJ, et al. **Intraindividual analysis of signal intensity changes in the dentate nucleus after consecutive serial applications of linear and macrocyclic gadolinium-based contrast agents.** *Invest Radiol* 2016;51:683–90 CrossRef Medline
28. Schweser F, Sommer K, Deistung A, et al. **Quantitative susceptibility mapping for investigating subtle susceptibility variations in the human brain.** *Neuroimage* 2012;62:2083–2100 CrossRef Medline
29. Wang Y, Spincemaille P, Liu Z, et al. **Clinical quantitative susceptibility mapping (QSM): biometal imaging and its emerging roles in patient care.** *J Magn Reson Imaging* 2017;46:951–71 CrossRef Medline
30. Haacke EM, Makki M, Ge Y, et al. **Characterizing iron deposition in multiple sclerosis lesions using susceptibility weighted imaging.** *J Magn Reson Imaging* 2009;29:537–44 CrossRef Medline
31. Bilgic B, Pfefferbaum A, Rohlfing T, et al. **MRI estimates of brain iron concentration in normal aging using quantitative susceptibility mapping.** *Neuroimage* 2012;59:2625–35 CrossRef Medline
32. Harder SL, Hopp KM, Ward H, et al. **Mineralization of the deep gray matter with age: a retrospective review with susceptibility-weighted MR imaging.** *AJNR Am J Neuroradiol* 2008;29:176–83 CrossRef Medline
33. Kanda T, Fukusato T, Matsuda M, et al. **Gadolinium-based contrast agent accumulates in the brain even in subjects without severe renal dysfunction: evaluation of autopsy brain specimens with inductively coupled plasma mass spectroscopy.** *Radiology* 2015;276:228–32 CrossRef Medline